JOURNAL OF MATERIALS SCIENCE 2 (1967) 313–323

An Investigation of Grain-Boundary Sliding during Creep

R. L. BELL
Engineering Laboratories, The University, Southampton, UK
T. G. LANGDON
University of California, Berkeley, California, USA

Received 1 November 1966, and in revised form 22 March 1967

A detailed experimental study of the behaviour of grain boundaries between surface grains has been carried out on a magnesium alloy, Magnox AL 80. Different methods of assessing the strain due to grain-boundary sliding were compared; the general agreement obtained confirmed the view that, under conditions of low stress and high temperature, sliding can play a very important role in the overall deformation.

1. Introduction

When metals are subjected to a stress greater than the elastic limit, the plastic strain which occurs is time-dependent. This thermally activated flow is called "creep". The processes contributing to creep include dislocation and vacancy movements, which give rise to changes in the dimensions of the grains, and "grain-boundary sliding" (i.e. relative displacements of the grains at the boundaries which separate them). The former processes are dominant at low temperatures, but above about 0.4 T_m (where T_m is the melting temperature of the metal in degrees Kelvin) grain-boundary sliding can make a significant contribution to the overall creep strain. In the present work, measurements were made to determine the importance of grain-boundary sliding in the creep of a magnesium alloy, Magnox AL80, over a range of temperatures and stresses.

2. Methods of Estimating the Strain due to Sliding

When two surface grains X and Y slide over each other, offsets are produced at the boundary in the manner shown in fig. 1. **AC** is the sliding vector, **u** is the component of sliding resolved along the stress axis, **v** is the component measured perpendicular both to the stress axis and to the specimen surface, and **w** is the component measured perpendicular to the stress axis but in the plane of the surface. Two angles define the

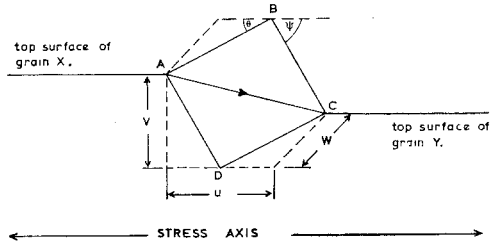

Figure 1 Schematic representation of grain-boundary sliding.

orientation of the grain boundary: θ, between the stress axis and the trace of the boundary in the plane of the surface; and ψ, the internal angle made by the boundary trace on a longitudinal section cut perpendicular to the surface. To obtain the elongation, ϵ_{gb}, due to the sliding at all the boundaries in a polycrystal, it is simplest, in principle, to sum the values of **u** measured at every boundary intersected by a line drawn parallel to the stress axis [1]. This sum may be expressed:

$$\epsilon_{gb} = \frac{1}{\mathbf{l}} \sum_{0}^{\mathbf{l}} \mathbf{u} \qquad (1)$$

where **l** is the length of the longitudinal traverse along which the offsets are summed. In practice, it is often difficult to measure these longitudinal offsets at the intersections of a longitudinal marker line with a grain boundary, owing to the

occurrence of grain-boundary migration. This trouble is avoided if **u** is measured from the displacement of a transverse marker. It then becomes convenient to make the summation along a transverse line [1], but, since a line tends to interest more boundaries that are normal to it, the transverse traverse is not representative of a longitudinal traverse. Equation 1 must therefore be modified to:

$$\epsilon_{gb} = \frac{1}{\mathbf{t}} \sum_{0}^{t} \mathbf{u} \tan \theta \qquad (2)$$

where **t** is the length of the transverse. This formula holds strictly only when the grains are equiaxed [2].

Alternatively, values of **u** may be obtained via measurements of **v**, **w**, θ, and ψ [3]. Equation 1 then becomes

$$\epsilon_{gb} = \frac{1}{\mathbf{l}} \sum_{0}^{l} \left(\frac{\mathbf{v}}{\tan \psi} + \frac{\mathbf{w}}{\tan \theta} \right)$$

$$= \frac{1}{\mathbf{l}} \left(\sum_{0}^{l} \frac{\mathbf{v}}{\tan \psi} + \sum_{0}^{l} \frac{\mathbf{w}}{\tan \theta} \right) \qquad (3)$$

For any pair of surface grains, **v** and **w** have a distinct physical difference. This is to be expected, since the constraints imposed by neighbouring grains are different for sliding perpendicular and parallel to the surface. The experimental results presented later confirm this difference. In the interior of a specimen, however, the difference is simply one of definition of axes, and it follows that:

$$\sum_{0}^{l} \frac{\mathbf{v}}{\tan \psi} = \sum_{0}^{l} \frac{\mathbf{w}}{\tan \theta}$$

and

$$\epsilon_{gb} = \frac{2}{\mathbf{l}} \sum_{0}^{l} \frac{\mathbf{v}}{\tan \psi} = \frac{2}{\mathbf{l}} \sum_{0}^{l} \frac{\mathbf{w}}{\tan \theta} \qquad (4)$$

In practice, this relation is useful only if an internal marker technique is available [4-6] to enable the offsets to be measured at interior boundaries.

The double summation (3) required at the surface is not easy to carry out, as it involves the measurement of an internal angle. Since **v** is by far the most convenient parameter to measure, and involves no damage to or treatment of the surface, the following relation due to Gifkins [7] is often used:

$$\epsilon_{gb} = \frac{k}{xd} \sum_{0}^{x} \mathbf{v} \quad \text{or} \quad \frac{k}{d} \times \bar{\mathbf{v}}_{ran} \qquad (5)$$

Here, k is a geometrical averaging factor, d is the grain diameter, and $\bar{\mathbf{v}}_{ran}$ is the average value of **v** on x randomly chosen boundaries.

It is customary to indicate the importance of the strain due to sliding by expressing it as a percentage of the total creep strain, viz. $100\ \epsilon_{gb}/\ \epsilon_t$. This quantity is named γ.

3. Materials and Experimental Procedure

The material used in this investigation was Magnox AL 80, a Mg/0.78 wt % Al alloy, whose spectrographic analysis is given in table I. It was supplied in the form of 1.27 cm diameter rod by Magnesium Elektron Ltd, Manchester. The rod had been produced by a 410° C two-stage extrusion process from a billet of 30.5 cm diameter, so that there was a strong tendency for grains to have their basal planes aligned parallel to the axis of the rod. The average grain diameter was 0.006 to 0.008 cm, the dimension in the longitudinal direction being about 2 to 5% greater than that in the transverse.

TABLE I Spectrographic analysis of Magnox AL80 expressed in ppm.

Al	7800	Zn	70
Be	40	Cu	< 50
Ca	< 50	Mn	< 50
Fe	40	Sn	< 50
Si	< 80	Ni	< 20
	Mg	Balance	

Tensile specimens were prepared with two, parallel, longitudinal, flat faces each approximately 3 cm long. The worked layer was removed from these by careful grinding on emery paper, followed by a 2 h anneal at a temperature in the range 430 to 540° C. Different temperatures in this range were used to obtain a range of grain sizes. Before testing, the flats were lightly ground, polished on diamond paste, and then electropolished. The grain size determined by the linear intercept method showed no difference between surface and interior grains. Individual specimens within which the grains were of widely varying size were discarded.

Straining was carried out in Dennison Model T47E creep machines under conditions of con-

stant load. At temperatures up to 200° C, the tests were performed in air with the specimen surface protected by a thin film of silicone oil; at higher test temperatures, an argon atmosphere was used to prevent oxidation. All of the surface measurements described below were made by interrupting the tests and removing the specimen from the machine.

3.1. Measurement of **v**

At low strains, where the mean step height was less than 1 μm, measurements were made using a Zeiss Linnik interference microscope, with an accuracy on each reading of ± 0.06 μm. At greater mean step heights, measurements were made by focusing on either side of the boundary, using a microscope with a calibrated, fine focus. This technique gave an accuracy on each reading of ± 0.5 μm.

Vertical offsets were measured at 300 randomly selected boundaries, giving an accuracy on the mean of order $\pm 10\%$ at the 95% confidence level [8].

3.2. Measurement of **u** and **w**

Two methods were used for grain-boundary displacements in the plane of the surface. In early experiments, fine lines were scribed both parallel and perpendicular to the stress axis using a diamond stylus. In later work, a photographically printed grid was preferred [9].

4. Results

Table II summarises the test conditions for the nineteen specimens used and fig. 2 shows some typical creep curves.

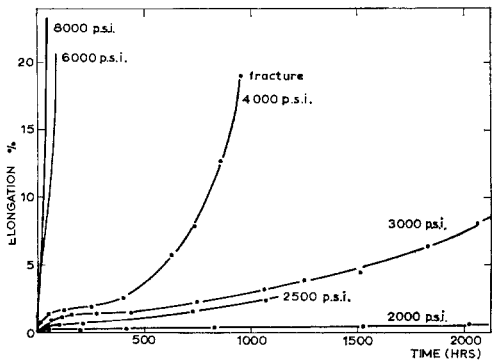

Figure 2 Creep curves for specimens with grain size ~0.01 cm tested at 200° C. (*Note* psi units are used in the illustrations; 1 psi ≡ 1 lb/in.^{2} = 7 × 10^{-2} kg/cm^2.)

An analysis of the secondary creep rates of all those specimens of grain size ~0.01 cm gave an activation energy Q of order 50 kcal/mole. To determine the stress exponent, n, a Zener-

TABLE II Summary of test conditions and results.

Specimen	No. of grains/cm	Stress (lb/in.^{2})†	Temperature (°C)	$\bar{v}_{ran}$ (at ϵ_t = 1%) (μm)	γ (at ϵ_t = 1%) (%)
MX 19*	100	8000	125	0.131	14
MX 21*	100	8000	150	0.159	17
MX 65	110	2000	200	0.644	75
MX 63	101	2500	200	0.581	63
MX 29	96	3000	200	0.584	60
MX 2	104	4000	200	0.566	63
MX 25*	104	6000	200	0.324	36
MX 31*	107	8000	200	0.131	15
MX 3	84	6000	200	0.334	30
MX 4	54	4000	200	0.935	54
MX 8	53	6000	200	0.370	21
MX 71	28	3000	200	1.536	46
MX 73	26	4000	200	1.065	30
MX 74	29	6000	200	0.408	12
MX 66	110	2000	250	0.544	64
MX 64	113	4000	250	0.281	34
MX 43*	108	2000	300	0.502	58
MX 26*	107	4000	300	0.227	26
MX 7	55	4000	300	0.493	29

*specimen repolished during test (at $\epsilon_t > 2\%$)
†1 lb/in.^{2} = 7 × 10^{-2} kg/cm^2

Hollomon plot [10] of temperature-compensated strain rate versus stress was made for those specimens having creep rates greater than 10^{-9} sec^{-1}. All these were within the range of conditions for which $Q = 50$ kcal/mole applied, and a value of $n \approx 7$ was obtained. This result agrees with that reported previously for Magnox tested under similar conditions, but the activation energy of 50 kcal/mole reported here is somewhat higher [14].

When the analysis was confined to data from tests at the lower end of both the stress and temperature ranges, the values indicated were $n \approx 5$ and $Q \approx 36$ kcal/mole.

Extensive non-basal slip was observed at the higher stresses, and, under these circumstances, similar high values of Q have been found for pure magnesium [11-13], but not previously for Magnox AL 80 [14]. It has been suggested that these values occur under conditions where prismatic slip is rate-controlling [11].

The value of Q obtained at the lower stresses is close to that for self-diffusion in magnesium (32 kcal/mole) [15], and the stress exponent $n = 5$ suggests that creep was limited by climb [13, 16]. But, it could be that the conditions were between those for an $n = 3$ process [14, 17] and the $n \approx 7$ process observed at the higher stresses.

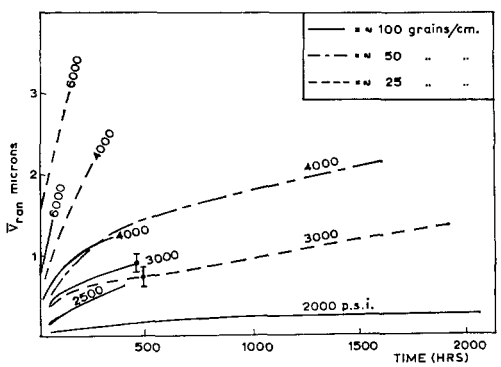

Figure 3 $\bar{v}_{ran}$/time curves for different stresses and grain sizes. All relate to a test temperature of 200° C.

4.1. v as a Function of Time

Fig. 3 shows the measurement of $\bar{v}_{ran}$ versus time for a number of specimens, all tested at 200° C. Comparison with fig. 2 shows that the shape of each of these curves is similar to that of the corresponding creep curve. In fact, $\bar{v}_{ran}$/elongation curves (fig. 4) are clearly resolved

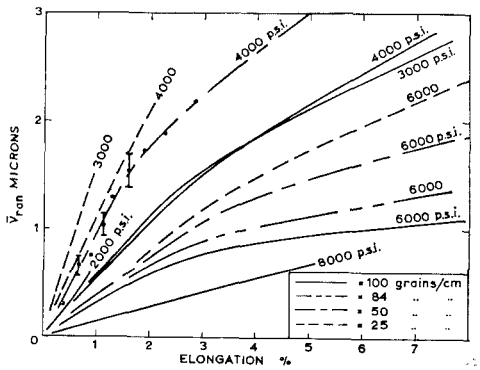

Figure 4 $\bar{v}_{ran}$/elongation curves for different stresses and grain sizes. All relate to a test temperature of 200° C.

into two parts: (i) an initial region in which $\bar{v}_{ran}$ increases linearly with strain; and (ii) a subsequent stage where $d^2\bar{v}_{ran}/d\epsilon_t^2$ is negative. The point of departure from the linear relationship follows no simple rule, but always occurs somewhere near the end of the secondary stage of creep.

Since, in general, the velocity of sliding decreased with time, it is not possible to describe the stress dependence of sliding velocity in a simple fashion. However, the velocity was approximately constant during secondary creep and, for different specimens of the same grain size tested at 200° C, it varied approximately as the fourth power of the stress. Analysis of the temperature dependence of sliding, again in the secondary creep region, gave an activation energy of 34 kcal/mole for specimens at 2000 lb/in.^{2} and 44 kcal/mole at 4000 lb/in.^{2} (1 lb/in.^{2} = 7×10^{-2} kg/cm^2).

In considering the effect of grain size on the sliding velocity of individual boundaries, one might expect that the greater distance between triple points in coarser-grained material would facilitate sliding. Fig. 3 shows agreement with this supposition, since the $\bar{v}_{ran}$/time curves for the coarser ~25 grains/cm specimens lie wholly above those for the finer ~100 grains/cm ones at stresses of 4000 and 6000 lb/in^2. In two other cases, there was an apparent reversal of this effect, if $\bar{v}_{ran}$ data for the whole of the creep curve were considered. However, restricting comparisons to the primary and secondary stages of creep, no significant exceptions to the general rule – that increased grain size gives greater sliding on individual boundaries – were found. To make this effect clear, the $\bar{v}_{ran}$ data relating

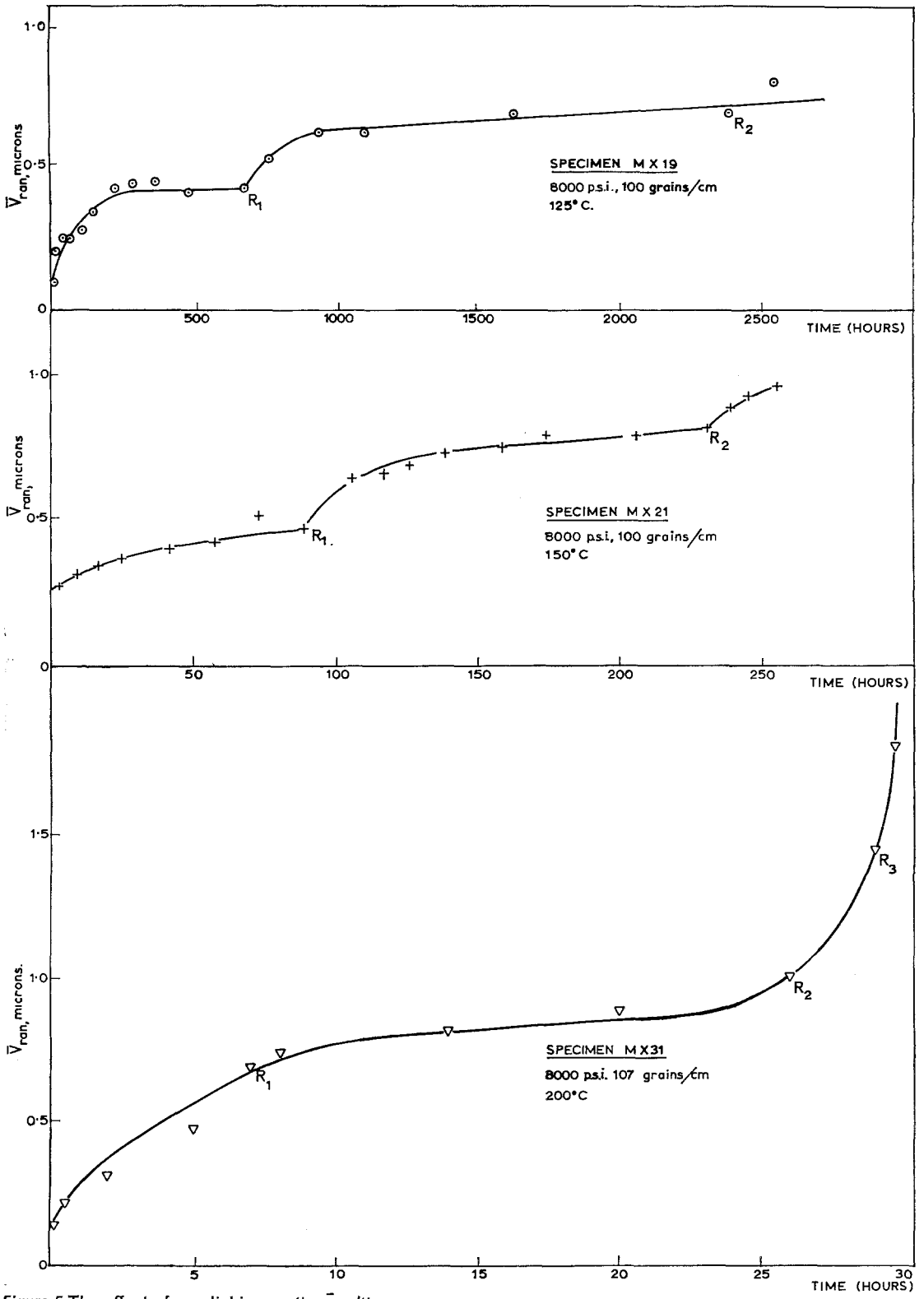

Figure 5 The effect of repolishing on the $\bar{v}_{ran}$/time curves.

to the tertiary stage of creep have been omitted from fig. 3.

4.1.1. The Effect of Repolishing

The specimens marked by an asterisk in table II were repolished during the course of the creep test. A depth of about 3 to 4 grains was removed from each of the flat surfaces, and the load was adjusted so as to restore the same tensile stress as that applied immediately before repolishing. The ensuing creep curve was a smooth continuation of that up to the point of repolishing, but in general there was a marked increase in the rate of sliding. Fig. 5 shows the experimental results for three different specimens. With specimens MX 19 and MX 21, repolishing operations were carried out at strains *beyond* the linear part of the $\bar{v}_{ran}$/elongation curve but before the onset of tertiary creep. In each case, there was a marked increase in the rate of sliding. Specimen MX 31 provided two kinds of exception to this behaviour: the first repolishing operation, R_1, was *during* the linear part of $\bar{v}_{ran}$ versus ϵ_t, and R_2, R_3, R_4 were in the tertiary stage of the creep curve. In none of these cases did repolishing affect $d\bar{v}_{ran}/dt$ (t = time).

Metallographic examination of specimens strained towards or beyond the end of the linear region revealed a striking difference between the appearance of grain boundaries at the surface and in the interior. At the surface (e.g. see fig. 6a), the boundaries connected triple points by an almost straight trace, but, with the removal of a layer of thickness half-a-grain-diameter or more, the boundary traces changed to an extremely irregular form. An exceptionally marked case of this is shown in fig. 6b, taken from the same specimen, at the same strain as in fig. 6a, but after the removal of a layer 3 to 4 grain-diameters thick. Corrugated boundaries were observed after each of the repolishing operations listed in table II. Similar corrugations were found in magnesium by Couling and Roberts [18] after creep tests at 149° C; although they found no corrugations at 315° C. Suiter and Wood [19] observed corrugations in magnesium tested at 200° C but not at 350° C. However, these involved much slower creep rates than the tests at 300° C reported here, where corrugations were seen.

4.2. The Topography of Surface Grains

Smith [20] showed that grain boundaries which intersect the free surface tend to become normal to it during annealing, and Gittins and Gifkins [21] have observed a similar effect during creep. In the present work, tests were carried out to examine more closely the effect of this migration on grain-boundary sliding at the surface.

4.2.1. Comparison of Cut and Annealed Surfaces.

Two, identical, electropolished specimens were annealed at 430° C for 2 h to give a grain size of 0.01 cm. The two plane surfaces of the one specimen were polished away ("cut") to a depth of about 5 grain-diameters; those on the other

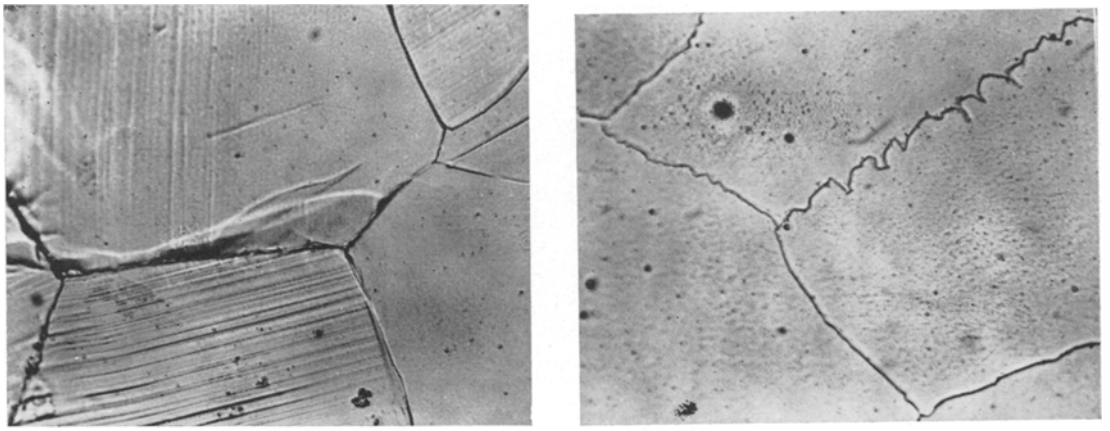

(a) (b)

Figure 6 Micrographs of specimen MX 31 after 5.18% strain (×390). (a) Grain-boundary configuration at the surface. (b) An exceptionally marked case of corrugated boundaries in the interior. This particular picture was obtained after removing a layer 3 to 4 grain-diameters thick.

("annealed") were untouched. Both specimens were sectioned perpendicular to these plane faces, and were polished and etched to reveal the grain-boundary configurations. Fig. 7 depicts a typical section normal to an "annealed" surface where a total of 400 readings of each of the angles ψ, α, and β were made; at the "cut" surface, only ψ measurements were taken.

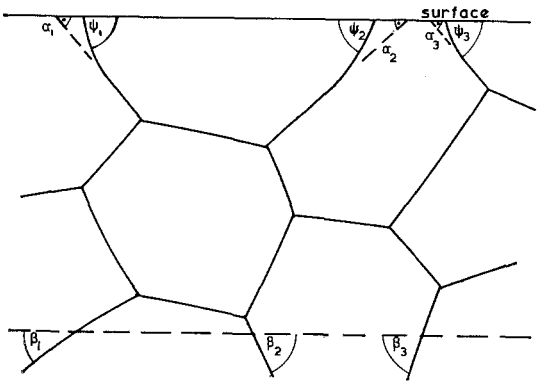

Figure 7 Transverse section of an annealed surface.

Fig. 8 presents the ψ values at the two kinds of surface in the form of histograms. At the "cut" face, the frequency of occurrence of a particular value of ψ was proportional to sin ψ, with a mean, $\bar{\psi}$, of 58°, which is very close to the value of 57.3° predicted by the application of Buffon's needle theorem [22]. At the "annealed" face, no values of ψ less than 35° were recorded and $\bar{\psi}$ was 77°. There was considerable curvature of the boundaries just below the surface, so that α, the angle made by that part of the boundary near to the first triple point, had an average value of only 61°. β, measured at a depth of two grains, had an average value of 59°, similar to that of the random distribution of the "cut" face.

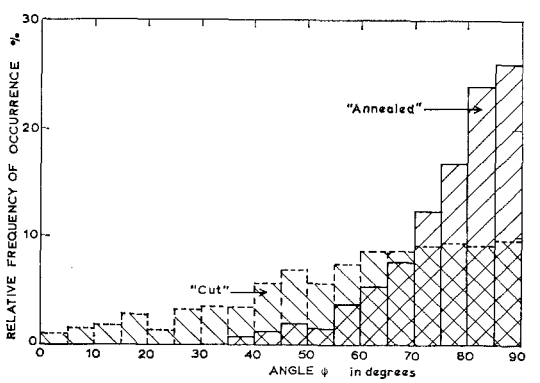

Figure 8 Histograms showing the frequency of occurrence of boundary-surface angle ψ on "cut" and "annealed" surfaces.

Measurements of ψ, on sections of specimens that had been annealed for 24 h at 200 and 300° C, gave values of $\bar{\psi}$ of 59.5 and 69.5° respectively. Thus, the anneal at 200° C produced no change, but the 300° C treatment produced a significant one, a fact which has been reported previously [19].

It should be noted that the histograms of ψ in fig. 8 do not give the distribution of the true angle ϕ made by the grain-boundary plane with the surface. Depending on the angle of section, ψ may take any value between ϕ and 0°. This problem has been treated in detail by Scriven and Williams [23], but their procedure was not carried out here.

4.2.2. Change of Surface-Boundary Angle during Creep

Two sets of electropolished specimens having a grain size of 0.01 cm were creep-tested at 200° C; one set at a stress of 4000 lb/in.^{2} and the other at 8000 lb/in^2. (The conditions were the same as those used for specimens MX 2 and MX 31 (of table II) respectively, and showed that creep curves were closely reproducible within the primary and secondary regions.) The tests were terminated at different strains and the specimens sectioned for determination of $\bar{\psi}$ values.

The results are shown in fig. 9. In both cases, $\bar{\psi}$ increased with strain from the original value of 58° to about 75°. Although this figure was first reached at a greater strain during creep at 8000 lb/in.^{2}, the elapsed time was only a fraction of that required at 4000 lb/in.^{2}; it is clear, therefore, that the stress played an important part. This point is further emphasised by the insertion on fig. 9 of the data for annealing at 200° C under zero stress.

It is suggested that the observed linearity between $\bar{v}_{ran}$ and extension during the initial stages of creep is connected with the change of the angle ψ that is taking place during this period, since the strain at which the sliding/extension curve deviates from linearity is approximately the same as that at which the internal angle tends to saturate.

4.2.3. $\bar{v}_{ran}$ versus Time with an "Annealed" Surface

Two specimens, MX 51 and MX 54, having similar grain sizes to MX 25 and MX 4 respect-

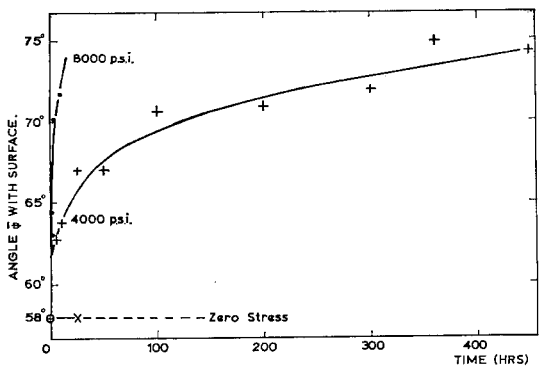

Figure 9 The change of the boundary-surface angle ψ as a function of time and creep stress.

ively, were tested under the same conditions, except that their surfaces were not electropolished after the pre-test anneal. The presence of the different surface-boundary configurations had no effect on the creep curve, but measurements of $\bar{v}_{ran}$ at intervals during the test showed quite a distinct behaviour.

The sliding rate at the annealed surface was considerably less than that at the as-cut surface (e.g. see fig. 10), but the $\bar{v}_{ran}/\epsilon_t$ curve was linear up to a much higher strain, although with a greatly reduced slope. Compared with as-cut specimens, the boundaries on the annealed ones showed very little migration.

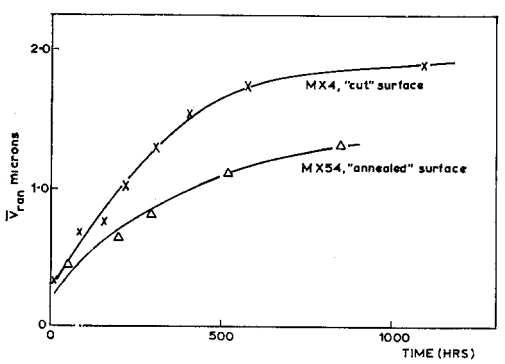

Figure 10 The effect of surface condition on the $\bar{v}_{ran}$/time curve. Both specimens of grain size ~0.02 cm, tested at 200° C, 4000 lb/in.^{2} (1 lb/in.^{2} = 7 × 10^{-2} kg/cm^2).

4.3. The Contribution of Sliding to the Creep Strain

Specimen MX 63 was used to make a careful check of the mutual consistency of the formulae developed in section 2. Two orthogonal sets of fine parallel lines were scribed on an electropolished surface before the test. Measurements of **u**, **v**, and **w** were made at a total strain of 2.49%. **u** was summed along a transverse traverse (e.g. see fig. 11), and **w** along a longitudinal one. In each case, 600 measurements were recorded with the corresponding values of θ. Values of **v** were summed both in random fashion and along a longitudinal traverse.

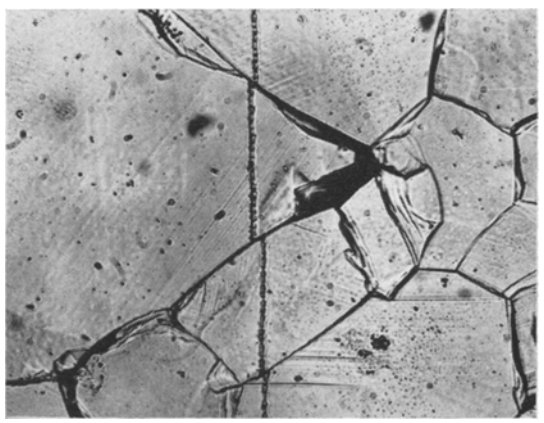

Figure 11 Offsets revealed by a transverse scribed marker on specimen MX 63 at 2.49% strain, stress axis horizontal (×260).

In the case of **u** and **w** measurements, it is possible to discriminate between sliding displacements which contribute to the creep elongation and those which are in the opposite sense. It was found that about 3% of the boundaries showed these negative offsets. They were usually small and identifiable with grain rotation.

Table III summarises the main results of this investigation. The values of γ obtained from **u** and **v** agree very well; the value from **w** comes within the error bracket of γ obtained from **v** but is just outside that from **u**. This is not surprising, since formula 4 makes no distinc-

TABLE III The contribution of sliding to the total creep strain in specimen MX 63.

Parameter measured	Formula used to obtain ϵ_{gb}	γ (%)
u	(2)	44 ± 6
v	(5) with k = 1.07*	49 ± 5
w	(4)	58 ± 7

*k value obtained empirically [24]

tion between the v and w components and, therefore, applies strictly only in the interior of a specimen. This point was brought out experimentally by measurements of v along a longitudinal traverse. The average of v summed in this way was 1.204 μm, compared with a w average, also taken on a longitudinal traverse, of 0.967 μm. In the interior, these quantities would be the same. (It should be noted that the v measurements referred to in table III were taken randomly. Their average was 1.144 μm.)

The value of k used in formula 5 was obtained experimentally by using the photographically printed grid technique to measure the grain strain, and hence, by difference with the total strain, determining that due to boundary sliding. The value $k = 1.07$ is the average of several closely similar figures obtained from independent measurements, which were all made at a total strain of 2%. Full details of this work will be published shortly [24].

To illustrate the effect of stress, temperature, and grain size on γ, formula 5 has been used (with $k = 1.07$) to give the results listed in the final column of table II. These values refer to a total strain of 1%, which in all cases is within the linear region of the corresponding $\bar{v}_{ran}/\text{elongation}$ curve. Fig. 12 shows clearly the effects of stress and grain size on γ at a fixed temperature (200° C). For a given grain size and stress, γ decreased with increasing temperature in the range 200 to 300° C.

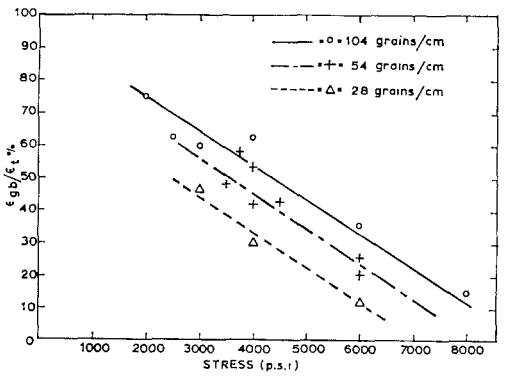

Figure 12 ϵ_{gb}/ϵ_t as a function of stress and grain size. All tests at 260° C.

5. Discussion

5.1. The Special Nature of the Sliding between Surface Grains

During creep, the boundaries between grains at a "cut" surface migrate to positions approximately normal to the free surface. The effect of this is two-fold. On the one hand, there is a progressive reduction in the resolved shear stress across the boundary. This would be expected to reduce the rate of sliding. On the other hand, the increase of ψ will give a greater increment Δv for each successive increment of sliding. Given that the resolved shear stress is rate-controlling, it can be shown [25] that the first of these two effects dominates and therefore dv/dt should decrease with increasing creep strain. This agrees with the experimental observations.

A difficulty arises, however, when values of $\bar{v}_{long}$ and $\bar{w}_{long}$ are compared (section 4.3). Both v and w represent components of sliding measured perpendicular to the stress axis. In the interior, their average values would be the same, but, because of the reduction in dv/dt noted above, at the surface one would expect v < w for any finite strain. The experimental result showed the inequality to be in the reverse direction. As this feature has been noticed in other independent experiments [25], it seems important to seek the reason. One possibility is that the large initial value of dv/dt is due to the lack of constraint perpendicular to the surface. This postulate alone is not adequate; it does not account for the observed difference in sliding rates on "cut" and "annealed" surfaces, nor for the effect of repolishing. The answer, it is suggested, lies in the extra driving force for migration provided by the tendency of grain boundaries to move to positions at right-angles to a free surface. In the interior, boundary corrugations were far more pronounced and clearly constituted a hindrance to sliding. At the surface, the boundaries "swept up" these currugations in moving round to positions normal to the surface. Hence, sliding rates were greater on a "cut" surface than on an "annealed" one, where the boundaries were already in an equilibrium situation. Repolishing gave rise to a resurgence of rapid sliding if it was carried out when the boundaries had reached the equilibrium position (i.e. after the end of the linear region in the $\bar{v}_{ran}/\epsilon_t$ curve) and therefore when the extra driving force for migration had vanished. The exposure of a new surface during tertiary creep (e.g. repolishing points R_2, R_3, R_4 in specimen MX 31) was ineffective, presumably because the corrugations were too firmly locked in place by this stage. Repolishing during the linear region of $\bar{v}_{ran}$ versus ϵ_t (e.g. R_1 on

MX 31) produced no acceleration of sliding because the extra driving force due to migration was available before, as well as after, the re-polish.

5.2. Grain-Boundary Sliding – An Independent or Secondary Process?

It has been suggested [26] that grain-boundary sliding is not a primary process of deformation responsive to the macroscopic applied stress, but simply a means of accommodating the discontinuities in the grain strain. This view is untenable in the present case, where the sliding has been found to depend on the resolved shear stress on the boundary [25] and where values of γ of up to 75% were obtained. The question remains as to whether sliding is limited by the same process which determines the rate of strain within the grains, or by some other process.

It is clear that grain-boundary sliding is not a simple process to be thought of in terms of the relative motion of two, perfectly flat, smooth surfaces. Real grain boundaries are rugged both on an atomic and on a microscopic scale, and sliding must involve migration and/or slip. The question is whether one of these processes or the intrinsic resistance of the boundary is rate-limiting in a particular situation. An attempt was made to settle this point for the present case, where the sliding rate during steady-state creep was obtained as a function of temperature and stress *from surface measurements* of $\bar{v}_{ran}$. At the lower stress levels, the activation energy for sliding ($Q \sim 34$ kcal/mole) was, within the limits of measurement, equal to that found for total creep ($Q \sim 36$ kcal/mole – which is close to that for self-diffusion). At the higher stresses, Q for sliding (44 kcal/mole) was slightly less than that for total creep (50 kcal/mole – which is equal to Q for prismatic slip); but the difference is not sufficient to identify positively a different rate-controlling process.

The stress exponent for sliding at 200° C ($n \approx 4$) was slightly smaller than that for total creep at this temperature ($n = 5$). Again, the difference was too small to draw firm conclusions about a difference of mechanism, but the result may be significant in that it is paralleled by the behaviour of lead bicrystals [27].

Earlier workers have suggested that a linear $\bar{v}/\epsilon_t$ curve is indicative of a common rate-controlling process in slip and sliding. The present results suggest that this linearity may hold only during the period when the grain boundaries on a cut surface are rotating to positions normal to the surface.

5.3. The Effect of Stress, Temperature, and Grain Size on γ

Although the stress and temperature dependence of sliding were not sufficiently different from those for total creep to enable separate rate-controlling processes to be identified, the small differences in n and Q were clearly manifest in a decrease of γ with increase of temperature (at constant stress) and an increase of γ with decrease of stress (at constant temperature).

The effect of stress noted here is the one normally observed; the effect of temperature is the reverse. However, in many previous experiments, the variables have not been properly separated and comparisons are of little value.

The effect of grain size on γ is most important because it is the most readily controlled metallurgical variable. Table II shows that, at constant stress and temperature, γ increased with a decrease in grain size, although the amount of sliding per boundary at any given strain was actually reduced. The increase in secondary creep rate, associated with a certain reduction in grain size, was too large to be accounted for entirely in terms of an increase in γ. In other words, grain size has an influence on the creep rate due to both crystal and boundary processes [28].

6. Conclusion

Measurements of the average grain-boundary offset, $\bar{v}_{ran}$, occurring perpendicular to the surface of specimens subjected to creep-testing, were shown to increase linearly with increasing strain, up to a total strain in the range 1 to 6%, and thence to increase at a slower rate. The strain at which the deviation from linearity occurred was found to be stress-dependent, such that it occurred at a higher strain for increasing stresses. Repolishing of specimens after the end of the linear region gave enhanced sliding perpendicular to the surface, and the occurrence of a second linear portion.

This effect was shown to be closely associated with the average internal angle $\bar{\psi}$ made by the boundaries with the surface, since the boundaries migrated during creep to positions of lower energy configuration perpendicular to the surface. The strain at which the saturation angle was attained was stress-dependent, and closely related to the point at which the sliding/exten-

sion curve ceased to be linear.

Under conditions of small grain size and slow rate of strain, it was found that sliding may account for up to 70 to 80% of the total deformation during the early stages of creep, up to about 2% total strain, and it seems probable that even larger contributions could be attained at slower rates. Strictly, these remarks apply only to surface behaviour, but it has been shown recently [2] that, in the interior, the γ values are not very different. It is therefore clear that grain-boundary sliding can be an important mode of deformation in metals subjected to creep at temperatures greater than about 0.4 T_m.

Although sliding was found to be dependent on the resolved shear stress acting along a boundary, it appears that the atomic process limiting the rate of sliding is the same as the one limiting slip within the grains.

Acknowledgements

The authors are indebted to Professor J. G. Ball for the provision of laboratory facilities in the Metallurgy Department, Imperial College, London, where the experimental work was performed. Grateful thanks are also extended to Dr R. C. Gifkins and Dr C. Graeme-Barber for many helpful discussions. The research was supported by a contract furnished by the United Kingdom Atomic Energy Authority.

References

1. H. BRUNNER and N. J. GRANT, *Trans. AIME* **215** (1959) 48.
2. C. GRAEME-BARBER, Ph.D. thesis, University of London (1967).
3. A. GITTINS, Ph.D. thesis, University of Melbourne (1964).
4. W. A. RACHINGER, *J. Inst. Metals* **81** (1952-53) 33.
5. Y. ISHIDA, A. W. MULLENDORE, and N. J. GRANT, *Trans. AIME* **233** (1965) 204.
6. C. GRAEME-BARBER and R. L. BELL, *J. Inst. Metals* **93** (1964-65) 551.
7. R. C. GIFKINS, "Fracture", edited by B. L. Averbach *et al* (MIT and John Wiley, 1959), p. 579.
8. A. GITTINS, M. Eng. Sc. thesis, University of Melbourne (1962).
9. R. L. BELL and T. G. LANGDON, *J. Sci. Instr.* **42** (1965) 896.
10. C. ZENER and J. H. HOLLOMON, *Trans. ASM* **33** (1944) 163; *J. Appl. Phys.* **15** (1944) 22.
11. S. A. DURAN, private communication.
12. W. J. MCG. TEGART, *Acta Met.* **9** (1961) 614.
13. R. B. JONES and J. E. HARRIS, *Proc. Joint Int. Conf. on Creep*, Inst. Mech. Eng., London (1963), paper 15.
14. *Idem*, CEGB Report No. RD/B/R.144 (July 1963).
15. P. G. SHEWMON and F. N. RHINES, *Trans. AIME* **200** (1954) 1021.
16. J. WEERTMAN, *J. Appl. Phys.* **28** (1957) 362.
17. *Idem, ibid*, 1185; *Trans. AIME* **218** (1960) 207.
18. S. J. COULING and C. S. ROBERTS, *Trans. AIME* **209** (1957) 1252.
19. J. W. SUITER and W. A. WOOD, *J. Inst. Metals.* **81** (1952-53) 181.
20. C. S. SMITH, *Trans. AIME* **175** (1948) 15.
21. A. GITTINS and R. C. GIFKINS, *Metals Sci. J.* **1** (1967) 15.
22. E. CZUBER, "Geometrische Wahrscheinlichkeiten und Mittelwerte" (B. G. Teubner, Leipzig, 1884), p. 84.
23. R. A. SCRIVEN and H. D. WILLIAMS, *Trans. AIME* **233** (1965) 1593.
24. R. L. BELL and T. G. LANGDON, to be published.
25. R. C. GIFKINS, R. L. BELL, A. GITTINS, and T. G. LANGDON, to be published.
26. A. W. MULLENDORE and N. J. GRANT, *Trans. AIME* **227** (1963) 319.
27. P. R. STRUTT, A-M LEWIS, and R. C. GIFKINS, *J. Inst. Metals.* **93** (1964-65) 71.
28. D. MCLEAN, "Mechanical Properties of Metals" (John Wiley, 1962), p. 307.